# The hysteretic voltage gap for a single-electron dual-junction-array trap with stray capacitances



2001 J. Phys.: Condens. Matter 13 9535

(http://iopscience.iop.org/0953-8984/13/42/313)

INSTITUTE OF PHYSICS PUBLISHING JOURNAL OF PHYSICS: CONDENSED MATTER

J. Phys.: Condens. Matter **13** (2001) 9535–9545 PII: S0953-8984(01)20692-4

# The hysteretic voltage gap for a single-electron dual-junction-array trap with stray capacitances

**Sang Chil Lee**[1], **Jai Yon Ryu**[1], **Doo Chul Kim**[1], **Dong Shik Kang**[1] **and Suck Whan Kim**[2]

[1] Department of Physics, Cheju National University, Cheju 690–756, Korea
[2] Department of Physics, Andong National University, Andong 760-749, Korea

Received 10 January 2001, in final form 17 May 2001
Published 5 October 2001
Online at stacks.iop.org/JPhysCM/13/9535

**Abstract**

The hysteretic voltage gap $\Delta V(m)$—the difference between the threshold voltages for single-charge-soliton tunnelling into and escape from a single-electron dual-junction-array trap (which consists of $2N$ gated small junctions with equal junction capacitances $C$, equal stray capacitances $C_0$, equal input gate capacitances $C_1$, and coupling capacitance $C_C$) through an $m$-junction cotunnelling process—is investigated for various charge solitons including a single electron, an exciton, and a combined soliton. Our results show that $\Delta V(m)$ has a strong dependence on $m$, $C_0/C$, $C_1/C$, $C_C/C$, and $N$, and that no hysteresis loop exists beyond a critical value $\eta_c$ of $C_0/C$. For finite stray capacitance and strong coupling capacitance, the exciton can be a candidate for use in constructing more stable single-electron circuits, as in the case of no stray capacitance and weak coupling capacitance previously discussed in the literature.

Correlated single-electron tunnelling phenomena based on the Coulomb blockade effect in nanostructures have been attracting wide attention. A lot of progress has been made [1–5] on the physics of single-electron tunnelling (SET) phenomena and on a wide variety of SET device applications. One system of interest to us is the single-electron dual-junction-array trap, which is composed of two capacitively coupled normal traps as shown in figure 1. In this system, the currents in the left and right arrays flow in a highly correlated manner because charge transport in the system is strongly affected by electrostatic coupling. Recently, Amakawa, Fujishima, and Hoh [5] studied the charge transport in such a system by using computer simulation taking into account cotunnelling, based on the tunnelling rate obtained from the approximation proposed by Fonseca *et al* [6]. However, their study is restricted to the case of the small-coupling-capacitance region, i.e. $C_C/C < 1$, where $C_C$ and $C$ are the coupling capacitance and the junction capacitance, respectively. Therefore, there are still some important questions which remain unanswered for the large-$C_C$ region. In addition, the role of the stray capacitance, which

0953-8984/01/429535+11$30.00  

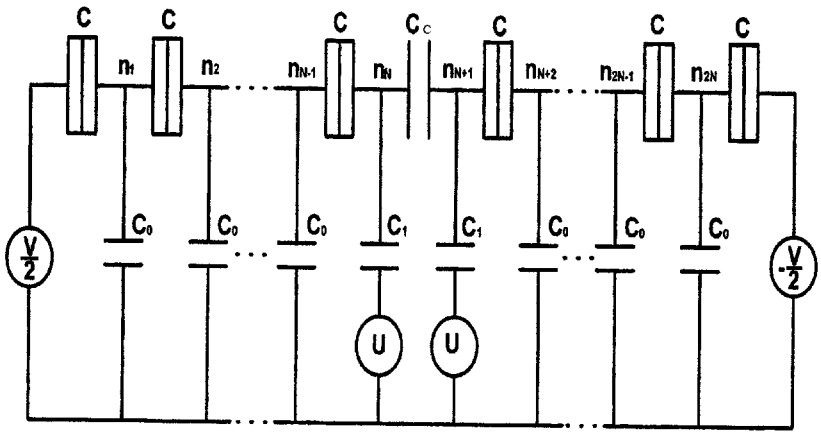


**Figure 1.** The single-electron dual-junction-array trap with $2N$ small junctions, with equal junction capacitances $C$, equal stray capacitances $C_0$, equal input gate capacitances $C_1$, and coupling capacitance $C_C$. The bias voltages of the two edges are $V/2$ and $-V/2$, while the voltages in the middle are $U$.

is known to be important in determining the soliton width in a one-dimensional (1D) array, has not been fully explored. The purpose of this study is to present the hysteretic voltage gaps of the single-electron dual-junction-array trap consisting of equal stray capacitances $C_0$, equal junction capacitances $C$, equal input gate capacitances $C_1$, and coupling capacitance $C_C$ for various charge-transfer processes (a single electron, a single exciton, and a combined soliton), on the basis of the exact analytical solution to the electrostatic problem of the single-electron dual-junction-array trap presented in the previous work [7], and to analyse them according to the parameters contained in the system. In particular, we are interested in the effect of the stray capacitance of the hysteretic voltage gap.

The starting point here is the Gibbs free energy, which can be written as [7]

$$F = E_{ch} - \frac{e^2}{2C}\sum_{i,j=1}^{2N} n_i H_{ij} n_j - \frac{1}{2}VQ_0 + \frac{1}{2}VQ_{2N+1} - UQ_N^g - UQ_{N+1}^g \qquad (1)$$

where $V$ is the bias voltage, $U$ is the gate voltage on the input gate capacitance, $n_i$ is the number of excess electrons on the $i$th island, and $H_{ij}$ is a matrix element which depends on $C_0$, $C$, $C_1$, and $C_C$. For detailed expressions for $E_{ch}$, $H_{ij}$, $Q_0$, $Q_{2N+1}$, $Q_N^g$, and $UQ_{N+1}^g$, we refer the reader to equations (19) and (20) in reference [7].

Equation (1) is a general expression for the Gibbs free energy of a single-electron dual-junction-array trap with bias voltage $\{V, U\}$ and charge profile $\{n_i e\}$ on the islands. On the basis of the Gibbs free energy (1), one can directly study the dynamics of the single-electron tunnelling by calculating the change of the Gibbs free energy $\Delta F$ due to some charge-transfer event. For definiteness, here we consider the three cases where the charge transfer was between two islands $k$ and $k'$, while the charges on the other islands are unchanged:

(i) the *single-charge-soliton (e)* case, where an electron is transferred from the $k$th island to the $k'$th island in the left-hand-side array (or the right-hand-side array);
(ii) the *exciton (electron–hole pair, e–h) case*, where an electron in the left-hand-side array is transferred from the $k$th island to the $k'$th island and an electron in the right-hand-side array is simultaneously transferred from the $(2N - k' + 1)$th island to the $(2N - k + 1)$th island;

(iii) the *combined-soliton (exciton–single-electron, ex–e) case*, where, in addition to the exciton case, an electron in the left-hand-side array is transferred from the $k'$th island to the $k''$th island.

We assume, however, that the tunnelling between two islands $N$ and $N+1$ is negligible, so we have two circuits that are independent galvanically but are coupled electrostatically [1]. We denote the charges on these islands before and after the charge transfer as $\{n_k, n_{k'}\}$ and $\{n'_k, n'_{k'}\}$, respectively, and the net transferred charges as $Q$, where $Q$ can be a single electron, an exciton, or a combined soliton. Under the above conditions, the change of the Gibbs free energy for the three cases of *charge-soliton transfer* can be derived from equation (1).

The tunnelling of a charge soliton from the $k$th island to the $k'$th island in the single-electron dual-junction-array trap is energetically favourable when the change of free energy $\Delta F^Q(k, k')$ is less than zero, and vice versa. Thus, the threshold energy $V_t$ for the transfer of a charge soliton from the $k$th island onto the $k'$th island can be obtained by equating $\Delta F^Q(k, k') = 0$. From equation (1), we obtain (for convenience, we take $U = 0$) for the *single-electron-transfer* case, the *exciton case*, and the *combined-soliton case*, respectively,

$$V_t^e(k, k') = \frac{e}{C}\frac{(H_{k'k'} - H_{kk})}{\delta_{0,k'} - \delta_{0,k} - \delta_{2N+1,k'} + \delta_{2N+1,k} - H_{1k'} + H_{2Nk'} + H_{1k} - H_{2Nk}} \tag{2}$$

$$\begin{aligned} V_t^{ex}(k, k') = {} & \frac{2e}{C}(H_{k'k'} - H_{k'2N-k'+1} - H_{kk} + H_{k2N-k+1}) \\ & \times \left[(\delta_{0,k} + \delta_{2N+1,2N-k+1} - \delta_{0,k'} - \delta_{2N+1,2N-k'+1}) \right. \\ & \left. + 2(H_{1k'} - H_{12N-k'+1} - H_{1k} + H_{12N-k+1})\right]^{-1} \end{aligned} \tag{3}$$

$$\begin{aligned} V_t^{ex-e}(k; k', k") = {} & \frac{2e}{C}(H_{k'k'} - H_{k'2N-k'+1} - H_{kk} + H_{k2N-k+1}) \\ & \times \left[(-\delta_{0,k'} - \delta_{2N+1,2N-k'+1} + \delta_{0,k} + \delta_{2N+1,2N-k+1}) \right. \\ & \left. + 2(H_{12N-k'+1} - H_{1k'} - H_{12N-k+1} + H_{1k})\right]^{-1}. \end{aligned} \tag{4}$$

Equations (2)–(4) enable us to immediately find the tunnelling and escape threshold voltages at $T = 0$ in the $m$-junction tunnelling sequence ($k \longleftrightarrow k+m$) for the *single-electron-transfer* case, the *exciton case*, and the *combined-soliton case*, respectively.

For the $m$-junction tunnelling events of the *single-electron-transfer* case, the tunnelling threshold voltage at $T = 0$ is given by $V_t^e(0, m)$ or $V_t^e(2N+1, 2N+1-m)$ because each absolute value is the largest for an electron tunnelling into the trap ($N$th island) of the left-hand-side array or the trap (($N+1$)th island) of the right-hand-side array, whereas the escape threshold voltage is given by $V_t^e(N, N-m)$ or $V_t^e(N+1, N+1+m)$ because each absolute value is the largest for an electron escaping from the trap ($N$th island) of the left-hand-side array or the trap (($N+1$)th island) of the right-hand-side array. In fact, $V_t^e(0, m)$ and $V_t^e(2N+1, 2N+1-m)$ for the tunnelling threshold voltage have identical magnitudes, and $V_t^e(N, N-m)$ and $V_t^e(N+1, N+1+m)$ for the escape threshold voltage are same as each other because the circuit is symmetric. As a result, the tunnelling and escape threshold voltages are, respectively, given by

$$V_t^e(0, m) = -\frac{e}{C}\frac{H_{mm}}{1 + H_{1m} - H_{2Nm}} \tag{5}$$

$$V_t^e(N, N-m) = \frac{e}{C}\frac{H_{N-mN-m} - H_{NN}}{\delta_{0,N-m} - H_{1N-m} + H_{N-m2N} + H_{1N} - H_{1N+1}} \qquad \text{for } 1 \leqslant m \leqslant N. \tag{6}$$

For the *exciton case*, the tunnelling and escape threshold voltages are, respectively, given by $V_t^{ex}(0, m)$ and $V_t^{ex}(N, N-m)$ because their absolute values are, respectively, the largest for an exciton tunnelling into the traps ($N$th and $(N+1)$th island) of both sides and for an exciton escaping from the traps, which are

$$V_t^{ex}(0, m) = \frac{e}{C}\frac{H_{mm} - H_{m2N-m+1}}{1 + H_{1m} - H_{12N-m+1}} \tag{7}$$

$$V_t^{ex}(N, N-m) = \frac{2e}{C}\frac{H_{N-mN-m} - H_{N-mN+1+m} - H_{NN} + H_{NN+1}}{-\delta_{0,N-m} - \delta_{2N+1,N+m+1} + 2(H_{1N-m} - H_{1N+m+1} - H_{1N} + H_{1N+1})}. \tag{8}$$

Similarly, the tunnelling and escape threshold voltages for the *combined-soliton case* are, respectively, given by $V_t^{ex-e}(0; m, N)$ and $V_t^{ex-e}(N; m, 0)$ because their absolute values are the largest for a combined soliton tunnelling into the trap and for a combined soliton escaping from the trap, which are, respectively, obtained as

$$V_t^{ex-e}(0; m, N) = \frac{e}{C}\frac{H_{mm} + H_{NN} - 2H_{mN+1}}{2 + H_{1m} + H_{1N} - H_{1N+1} - H_{12N-m+1}} \tag{9}$$

$$V_t^{ex-e}(N; m, 0) = -\frac{e}{C}\frac{H_{mm} - H_{NN} + H_{NN+1}}{1 - H_{1m} + H_{12N-m+1} + 2H_{1N} - 2H_{1N+1}}. \tag{10}$$

Equations (5)–(10) are general forms for the $m$-junction cotunnelling process, where solitons tunnel across $m$ junctions at the same time. When $m = 1$, it becomes the special case of one-junction tunnelling.

An interesting phenomenon associated with the multi-junction trap, as in the measured $I$–$V$ curves [8], is the hysteretic loop; i.e. the tunnelling and escape of a soliton do not occur at the same value of bias voltage $V$. Since we have obtained analytic expressions for the threshold voltages for both the tunnelling and escape of a single charge soliton in the single-electron dual-junction-array trap, we can now study the hysteretic phenomenon in a quantitative way. For this purpose, we introduce the hysteretic voltage gap $\Delta V$, which is defined as the difference between the threshold voltages for the tunnelling and escape of a soliton in the single-electron dual-junction-array trap. From this definition one can obtain the results for the hysteretic voltage gaps of a single electron, an exciton, and a combined soliton with cotunnelling transfer, respectively, as

$$\begin{aligned}\Delta V^{e}(m) &\equiv V_t^{e}(N, N-m) - V_t^{e}(0, m) \\ &= -\frac{e}{C}\left(\frac{H_{N-mN-m} - H_{NN}}{H_{1N-m} - H_{1N+m+1} - H_{1N} + H_{1N+1}} - \frac{H_{mm}}{1 + H_{1m} - H_{2Nm}}\right)\end{aligned} \tag{11}$$

$$\begin{aligned}\Delta V^{ex}(m) &\equiv V_t^{ex}(N, N-m) - V_t^{ex}(0, m) \\ &= \frac{e}{C}\left(\frac{H_{N-mN-m} - H_{N-mN+1+m} - H_{NN} + H_{NN+1}}{H_{1N-m} - H_{1N+m+1} - H_{1N} + H_{1N+1}} - \frac{H_{mm} - H_{m2N-m+1}}{1 + H_{1m} - H_{12N-m+1}}\right)\end{aligned} \tag{12}$$

and

$$\begin{aligned}\Delta V^{ex-e}(m) &\equiv V_t^{ex-e}(N; m, 0) - V_t^{ex-e}(0; m, N) \\ &= -\frac{e}{C}\left(\frac{H_{mm} - H_{NN} + H_{NN+1}}{1 - H_{1m} + H_{12N-m+1} + 2H_{1N} - 2H_{1N+1}}\right. \\ &\quad \left. + \frac{H_{mm} + H_{NN} - 2H_{mN+1}}{2 + H_{1m} + H_{1N} - H_{1N+1} - H_{12N-m+1}}\right)\end{aligned} \tag{13}$$

where $m$ denotes the number of junctions that the electrons tunnel across. The $\Delta V$ of equations (11)–(13) is a measure of the hysteretic effect for the *single-charge-soliton transfer* of the single-electron dual-junction-array trap. When $\Delta V > 0$, there is a difference between the threshold voltages for the escape and tunnelling of a charge soliton. After a charge soliton tunnels into the trap of system at a voltage above $V_t(0, m)$, the soliton cannot escape until the voltage is reduced to $V_t(N, N-m)$. Things are different at $\Delta V(m) < 0$, where a reduction of the voltage from $V_t(0, m)$ will immediately result in the escape of the soliton, i.e. the soliton cannot be trapped in the system. Thus, it is to be noted that when $\Delta V > 0$, the system can be used as a memory cell. There are two important things of interest to us in equations (11)–(13): one is which soliton has the largest hysteretic voltage gap and the other is how the hysteretic voltage gaps depend on the stray capacitance $C_0$, the input gate capacitance $C_1$, the coupling capacitance $C_C$, the cotunnelling $m$, and the number of junctions $N$. From the results obtained, we can get detailed information about the stability condition of the system and a candidate for use in constructing the most stable single-electron circuits. In fact, the analytical form of the stability condition can be obtained from the derivative of the hysteretic voltage gaps in equations (11)–(13) with respect to the parameters given in the system, but the results are not simple. So, the dependence of the hysteretic voltage gaps on the stray capacitance $C_0$, the input gate capacitance $C_1$, the coupling capacitance $C_C$, the cotunnelling $m$, and the number of junctions $N$ will be analysed numerically using equations (11)–(13). In the following, we study the dependence on $C_0$, $C_C$, $C_1$, and $m$ of $\Delta V(m)$, taking $N = 3$ as an example.

The stray-capacitance dependence of $\Delta V(1)$ (in units of $e/C$) for various charge solitons is illustrated in figure 2, where we plot the hysteretic voltage gap of equations (11)–(13) as a function of the ratio of the stray capacitance to the junction capacitance, i.e., $\eta$ ($\equiv C_0/C$) at $N = 3$, $m = 1$, and $\beta$ ($\equiv C_1/C$) $= 0.5, 1, 5$ for two different coupling capacitances: (a) $\alpha$ ($\equiv C_C/C$) $= 0.5$ and (b) $\alpha = 5$. As shown in figure 2(a), all charge solitons have their maximum values of hysteretic voltage gaps at $\eta = 0$ for weak coupling capacitance and all given $\beta$-values. In that case, the system becomes stable at $\eta = 0$ for weak coupling capacitance and all given $\beta$-values because it is very difficult for the solitons to escape from the trap of the system, as expected from the definition of $\Delta V$. It is shown that when the stray capacitance $\eta$ increases, the hysteretic voltage gaps of all charge solitons decrease, which is due to the decrease of the threshold voltages for the escape of charge solitons. Thus, the effect of the stray capacitance reduces the stability of the system. It is also shown for weak coupling capacitance that the single exciton is a candidate for use in constructing the most stable single-electron circuits, as suggested by Amakawa *et al* [5], because the exciton has larger hysteretic voltage gaps than any other charge solitons except for large $\eta$. Figure 2(b) shows that, for strong coupling capacitance and all given $\beta$-values, single electrons and combined solitons have their maximum values of hysteretic voltage gaps at $\eta = 0$ and their hysteretic voltage gaps decrease with increase of the stray capacitance $\eta$, as in figure 2(a), whereas the single excitons have their maximum values of hysteretic voltage gaps at a specific value of the stray capacitance. It is clearly seen from the figure that the single exciton is a candidate for use in constructing the most stable single-electron circuits, because the single exciton has larger hysteretic voltage gaps than any other charge soliton except for large $\eta$, as in figure 2(a). It is interesting to note that for weak coupling capacitance the most stable single-electron circuits are constructed in the absence of stray capacitance, whereas for strong coupling capacitance the most stable single-electron circuits are constructed in the presence of stray capacitance. If the stray capacitance is very large for all given values of $\alpha$ and $\beta$, the combined soliton has larger hysteretic voltage gaps than any other charge soliton, but the gaps are very small. So, no special attention will be paid to this case.

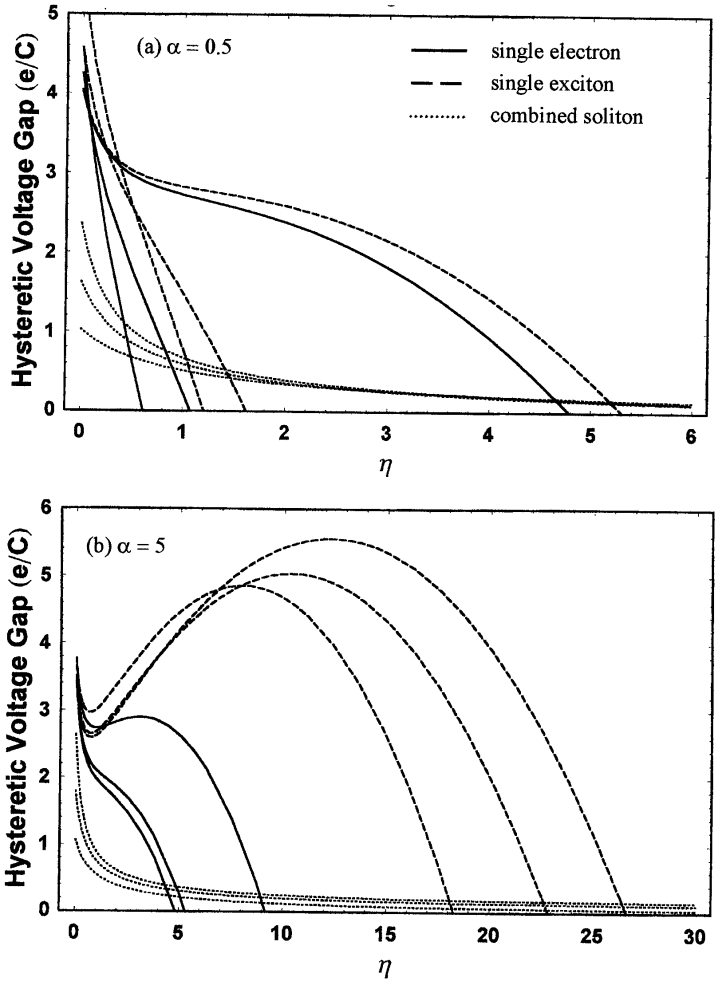


**Figure 2.** The hysteretic voltage gaps $\Delta V(1)$ (in units of $e/C$) of a single-electron dual-junction-array trap with $N = 3$ for various charge solitons, as a function of $C_0/C$ at (a) $C_1/C = 0.5, 1, 5$ (from the left-hand side to the right-hand side of the bottom part for solid lines and dashed lines, and from top to bottom of the left-hand side for dotted lines) for $C_C/C = 0.5$ and (b) $C_1/C = 0.5, 1, 5$ (from the left-hand side to the right-hand side of the bottom part for solid lines, from the right-hand side to the left-hand side of the bottom part for dashed lines, and from top to bottom of the left-hand side for dotted lines) for $C_C/C = 5$. Here $C_C$, $C_1$, $C$, and $C_0$ are the coupling capacitances, input gate capacitances, junction capacitances, and stray capacitances, respectively.

Another remarkable thing in figure 2 is that for all given values of $\alpha$ and $\beta$, the hysteretic voltage gaps of all charge solitons, except for the combined soliton, approach zero as the value of $\eta$ increases. For zero hysteretic voltage gap, the threshold voltages for the tunnelling and escape of the exciton are same and no hysteresis loop exists. In this case, the system cannot be used as a memory cell because one cannot ensure that all charge solitons are trapped in the system. As can be seen from the figure, the critical stray capacitances $\eta_c$ at which $\Delta V(1) = 0$ strongly depend on the values of $\alpha$ and $\beta$. For weak coupling capacitance, the critical stray capacitances of the single electron and single exciton increase with increase of the input gate capacitance. However, for strong coupling capacitance the critical stray capacitances of the

single electron increase with increase of the input gate capacitance whereas those of the single exciton decrease with increase of the input gate capacitance. Moreover, it is shown that for a fixed value of $\beta$ the critical stray capacitances of all charge solitons increase with increase of the coupling capacitance. The dependence of the critical stray capacitances on parameters given for the system can be readily obtained by putting $\Delta V(1) = 0$ in equations (11)–(13). The detailed investigation will be discussed later.

Figure 3 shows the coupling capacitance dependence of $\Delta V(1)$ (in units of $e/C$) for various charge solitons, where we plot the hysteretic voltage gap of equations (11)–(13) as a function of the ratio of the coupling capacitance to the junction capacitance, i.e., $\alpha$ ($\equiv C_C/C$) at $N = 3$,

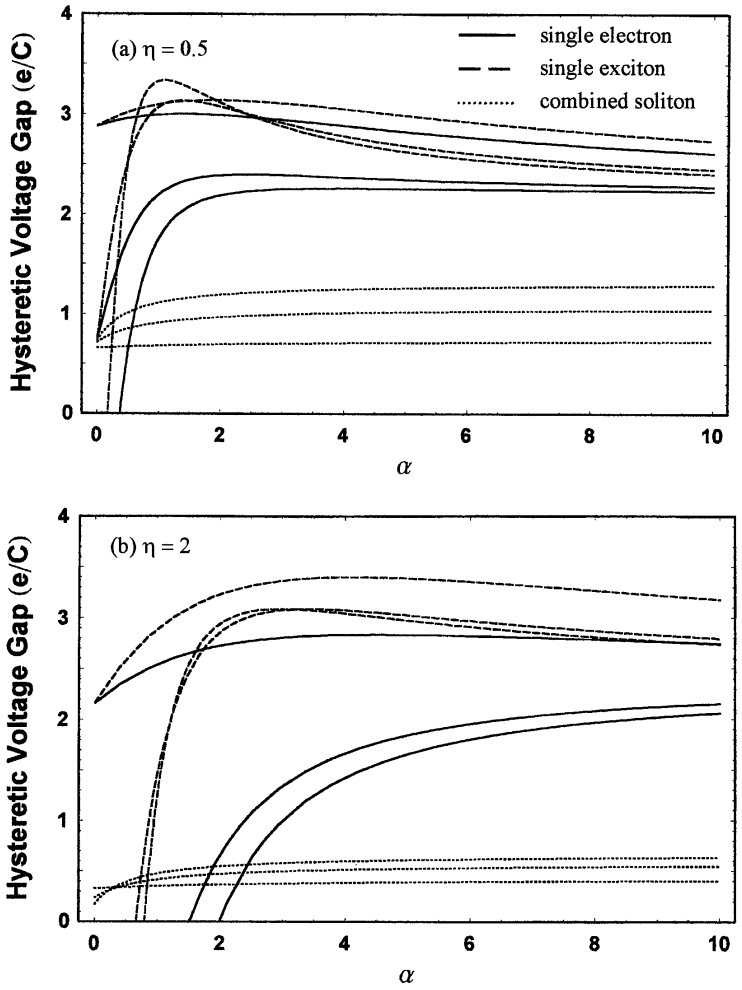


**Figure 3.** The hysteretic voltage gaps $\Delta V(1)$ (in units of $e/C$) of a single-electron dual-junction-array trap with $N = 3$ for various charge solitons, as a function of $C_C/C$ at (a) $C_1/C = 0.5$, 1, 5 (from bottom to top of the left-hand side for solid lines and dashed lines, and from top to bottom for the dotted lines) for $C_0/C = 0.5$ and (b) $C_1/C = 0.5$, 1, 5 (from bottom to top of the right-hand side for solid lines and dashed lines, and from top to bottom of the right-hand side for dotted lines) for $C_0/C = 2$. Here $C_C$, $C_1$, $C$, and $C_0$ are the coupling capacitances, input gate capacitances, junction capacitances, and stray capacitances, respectively.

$m = 1$, and $\beta$ ($\equiv C_1/C$) $= 0.5, 1, 5$ for two different stray capacitances: (a) $\eta$ ($\equiv C_0/C$) $= 0.5$ and (b) $\eta = 2$. It is clearly seen from figures 3(a) and 3(b) that the single exciton has larger hysteretic voltage gaps than any other charge soliton when the coupling capacitance becomes strong for all given values of $\beta$ and $\eta$, and that the hysteretic voltage gaps of all charge solitons decrease with increase of the stray capacitance, as in figure 2. Therefore, we can see that the single exciton is a candidate for use in constructing the most stable single-electron circuits, and that the effect of the stray capacitance reduces the stability of the system. When the coupling capacitance is very small for $\beta \leqslant 1$ and $\eta = 2$, the combined soliton has larger hysteretic voltage gaps than any other charge soliton, but the gaps are very small. So, no special attention will be paid to this case. The cotunnelling $m$-dependence of the hysteretic voltage gaps $\Delta V(m)$ (in units of $e/C$) for various charge solitons is shown in figure 4, where we plot the hysteretic voltage gap of equations (11)–(13) as a function of the cotunnelling $m$ at $\alpha = 0.5$, $\beta = 5$, and $N = 10$, for different stray capacitances: $\eta = 0.005, 0.05, 0.5$. It can be seen from the figure that the hysteretic voltage gaps of the single electron and single exciton at fixed values of $\alpha$, $\beta$, and $\eta$ decrease with increase of the cotunnelling $m$. This means that when the cotunnelling $m$ increases, the threshold voltages for the escape of the single electron and exciton decrease or those for the tunnelling of the single electron and single exciton increase. Thus, the effect of the cotunnelling reduces the stability of the system. Unlike in the cases for the single electron and exciton, the hysteretic voltage gaps of the combined soliton remain constant for given $\eta$ as the cotunnelling increases. It is to be noted that the changes of the hysteretic voltage gaps of single charge solitons depending on the cotunnelling $m$ can be understood from the changes of the free energy and the threshold voltage depending on the cotunnelling $m$.

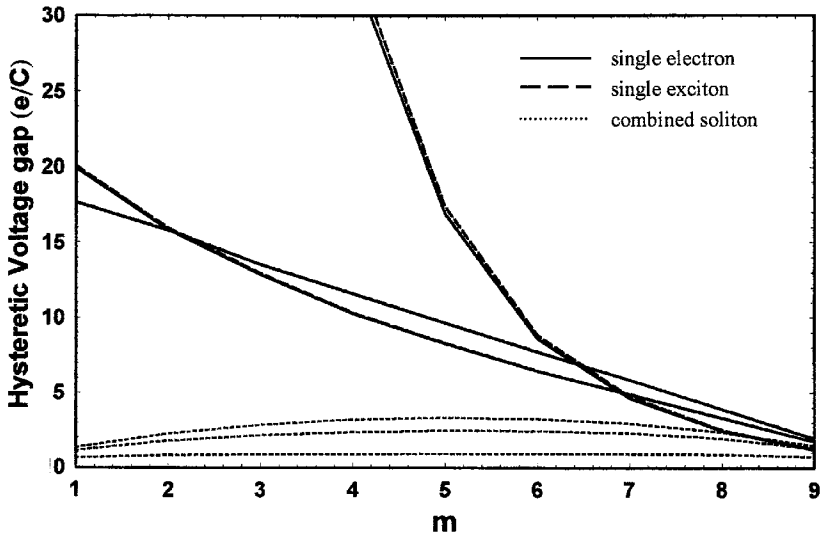


**Figure 4.** The hysteretic voltage gaps $\Delta V(1)$ (in units of $e/C$) of a single-electron dual-junction-array trap with $N = 10$ for various charge solitons, as a function of cotunnelling $m$ at $C_C/C = 0.5$ and $C_1/C = 5$ for $C_0/C = 0.005$, 0.05, and 0.5 (from top to bottom of the right-hand side). Here $C_C$, $C_1$, $C$, and $C_0$ are the coupling capacitances, input gate capacitances, junction capacitances, and stray capacitances, respectively.

Next, we study the dependence on $\alpha$, $\beta$, and $N$ of the critical stray capacitances ($\eta_c$) in more detail, taking $m = 1$ as an example. The dependence of the critical stray capacitances can be readily obtained by putting $\Delta V(1) = 0$ in equations (11)–(13), as discussed in relation

to figure 2. Since the analytical results for $\eta_c$ have complicated forms, we present some results numerically in the following. The general relationship between $\eta_c$ and $\alpha$ for various charge solitons is illustrated in figure 5, where we plot $\eta_c$ as a function of $\alpha$ at $\beta = 0.5, 1, 2$ for $N = 3$ and $m = 1$. It is clearly seen from the figure that the critical stray capacitances of all charge solitons increase slowly or rapidly with the increase of the value of $\alpha$ for all given $\beta$-values and that those of the single exciton and combined soliton have a more complicated dependence on the value of $\beta$ for fixed values of $\alpha$: in the small-$\alpha$ region, their critical stray capacitances increase with increase of the value of $\beta$. However, they decrease with increase of the value of $\beta$, except for in specific regions of $\alpha$, as the value of $\alpha$ increases. It is to be noted that the system cannot be used as a memory cell for every point above each line. The $N$-dependence of the critical stray capacitances for various charge solitons, for various values of $\beta$ at $\alpha = 0.5$ and $m = 1$, is presented in figure 6. It can be seen from the figure that for given $\alpha$ and $\beta$, the changes of the critical stray capacitances of all charge solitons are expected for $N < 3$ and they are not influenced by the number of junctions for $N \geqslant 3$, since they remain constant for increasing number of junctions. Moreover, for a fixed value of $N$, the critical stray capacitances for all charge solitons increase with increase of the value of $\beta$. It is to be noted that there is no hysteresis loop for every point above each line.

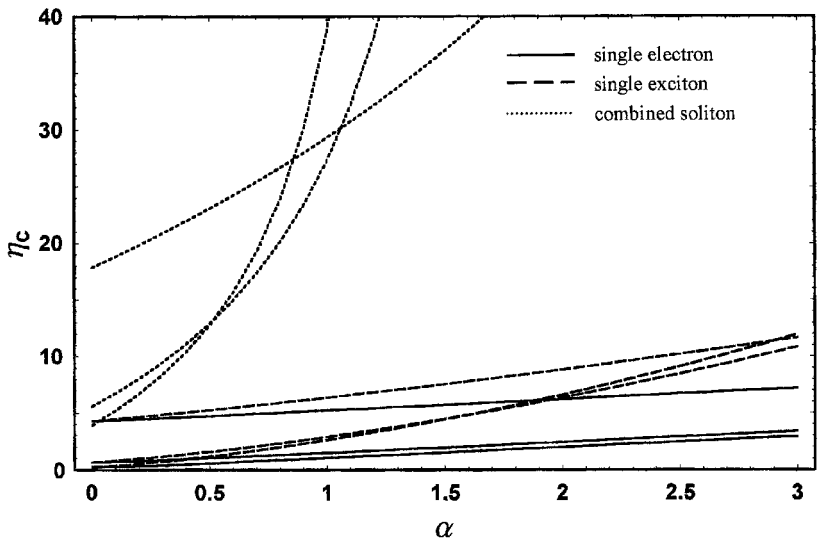


**Figure 5.** The critical value $\eta_c$ of $C_0/C$ at which $\Delta V = 0$ for various charge solitons, as a function of $C_C/C$ at $C_1/C = 0.5, 1, 2$ (from bottom to top of the left-hand side) for $m = 1$ and $N = 3$. Here, $N$ is the number of tunnelling junctions on each side of the single-electron dual-junction-array trap and $C_C$, $C_1$, $C$, and $C_0$ are the coupling capacitances, input gate capacitances, junction capacitances, and stray capacitances, respectively. For every point above each line there is no hysteresis.

So far, we have obtained the hysteretic voltage gaps of the single-electron dual-junction-array trap with equal stray capacitances for various charge solitons including a single electron, an exciton, and a combined soliton. With the analytical results obtained, we have performed a numerical analysis of the hysteretic voltage gaps, in order to understand their dependence on the stray capacitance, the coupling capacitance, the input gate capacitance, and the cotunnelling. In addition, we have investigated the dependence on $\alpha$, $\beta$, and $N$ of the critical stray capacitances ($\eta_c$) at which $\Delta V(1) = 0$ in equations (11)–(13). Unfortunately, we do not have any

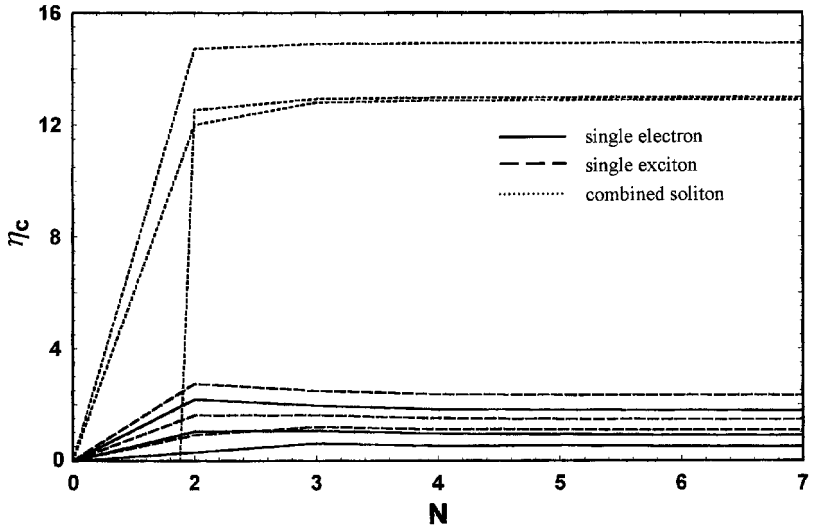


**Figure 6.** The critical value $\eta_c$ of $C_0/C$ for $\Delta V = 0$ for various charge solitons, as a function of $N$ at $C_1/C = 0.5, 1, 2$ (from bottom to top of the right-hand side) for $m = 1$ and $C_C/C = 0.5$. Here, $N$ is the number of tunnelling junctions on each side of the single-electron dual-junction-array trap and $C_C$, $C_1$, $C$, and $C_0$ are the coupling capacitances, input gate capacitances, junction capacitances, and stray capacitances, respectively. For every point above each line there is no hysteresis.

experimental results on the single-electron dual-junction-array trap, except for the numerical results of Amakawa *et al* [5] obtained for no stray capacitance and weak coupling and input gate capacitances. Our results show that the hysteretic voltage gaps strongly depend on the stray capacitance $C$, the input gate capacitance $C_1$, the coupling capacitance $C_C$, and the cotunnelling $m$. For weak coupling capacitance and all given $\beta$-values, all charge solitons have their maximum values of hysteretic voltage gaps at $\eta = 0$ and the hysteretic voltage gaps of all charge solitons decrease as the stray capacitance $\eta$ increases. It is shown for weak coupling capacitance that the single exciton is a candidate for use in constructing the most stable single-electron circuits, as suggested by Amakawa *et al* [5], because the exciton has larger hysteretic voltage gaps than any other charge solitons except for large $\eta$. For strong coupling capacitance and all given $\beta$-values, the single electron and combined soliton have their maximum values of hysteretic voltage gaps at $\eta = 0$ and their hysteretic voltage gaps decrease with increase of the stray capacitance $\eta$, as in the case of weak coupling capacitance. However, the single excitons have the maximum values of hysteretic voltage gaps at a specific value of the stray capacitance and they have larger hysteretic voltage gaps than any other charge soliton except for large $\eta$, as in the case of weak coupling capacitance. Thus, the single exciton is a candidate for use in constructing the most stable single-electron circuits. It is interesting to note that for weak coupling capacitance the most stable single-electron circuits are constructed in the absence of stray capacitance, whereas for strong coupling capacitance the most stable single-electron circuits are constructed in the presence of stray capacitance. Moreover, the hysteretic voltage gaps of all charge solitons are very sensitive to the cotunnelling effect. It is shown that the hysteretic voltage gaps of the single electron and single exciton at fixed values of $\alpha$, $\beta$, and $\eta$ decrease with increase of the cotunnelling $m$. However, the hysteretic voltage gaps of the combined soliton remain constant for given $\eta$ as the cotunnelling increases. It is to be noted that the changes of the hysteretic voltage gaps of single charge solitons depending on

the cotunnelling $m$ can be understood from the changes of the free energy and the threshold voltage depending on the cotunnelling $m$. In addition, the critical stray capacitances in which no hysteresis is expected depend on the coupling capacitor $C_C$, the junction capacitance $C$, the input gate capacitance $C_1$, and the number of junctions, as well as the cotunnelling.

In conclusion, the hysteretic voltage gaps are very sensitive to the stray capacitance $C$, the input gate capacitance $C_1$, the coupling capacitance $C_C$, the cotunnelling $m$, and the number of junctions $N$. A single exciton can be a candidate for use in constructing more stable single-electron circuits, depending on the parameters of the system. We expect the quantitative and qualitative behaviours investigated in this paper to provide useful information pertinent to future experiments.

## Acknowledgment

This work was supported by the Korea Research Foundation (No 1998-016-E00089).

## References

[1] Averin D V, Korotkov A N and Nazarov Yu V 1991 *Phys. Rev. Lett.* **66** 2818
[2] Grabert H and Devoret M H (ed) 1992 *Single Charge Tunneling (NATO ASI Series B)* (New York: Plenum) p 217
[3] Averin D V and Odintsov A A 1989 *Phys. Lett.* A **140** 251
[4] Hu G Y and O'Connell R F 1996 *Phys. Rev.* B **54** 1522
[5] Amakawa S, Fujishima M and Hoh K 1996 Dual-junction-array single electron trap *The Electrochemical Society October Meeting* vol 2 (Princeton, NJ: The Electrochemical Society) p 572
[6] Fonseca L R C, Korotkov A N, Likharev K K and Odintsov A A 1995 *J. Appl. Phys*. **78** 3238
[7] Ryu J Y, Lee S C, Hu G Y and Ting C S 2000 *J. Phys. C: Solid State Phys.* **12** 4641
[8] Dresselhaus P D, Ji L, Han S, Lukens J E and Likharev K K 1994 *Phys. Rev. Lett.* **72** 3226